STUDIA UBB CHEMIA, LXII, 3, 2017 (p. 187-195)
(RECOMMENDED CITATION)
DOI:10.24193/subbchem.2017.3.15

***In memory of prof. dr. Simion Gocan***

# ENHANCEMENT OF PHYSICAL PROPERTIES IN $ZrO_2/Ga_2O_3$ CO-SUBSTITUTED INDIUM OXIDE

**LILIANA BIZO[a *], ADRIANA VULPOI[b], FIRUŢA GOGA[a]**

**ABSTRACT.** The effect of coupled substitution of $Zr^{4+}/Ga^{3+}$ for $In^{3+}$ in $In_2O_3$ upon the structural, electrical and optical properties has been studied. The $In_{2-2x}Ga_xZr_xO_3$ solid solution with bixbyite structure has been synthesized for $0 \leq x < 0.15$. A decrease in resistivity for the composition $x = 0.025$ ($\rho_{RT} = 5.5x10^{-3}$ Ω.cm) by approximately one order of magnitude if compared to $In_2O_3$ ($\rho_{RT} = 2.2x10^{-2}$ Ω.cm) was obtained. The maximum percent reflectance around 500 nm is lowered by 15% with respect to pure $In_2O_3$. These novel oxides show their potential as transparent conductors.

***Keywords:*** *transparent conducting oxides, solid state reaction, electrical conductivity, optical properties.*

## INTRODUCTION

The simultaneous presence of optical transparency and electronic conductivity in metal oxides produces a special class of materials, transparent conducting oxides (TCOs). These materials are suitable for a wide range of applications, such as sensors, solar cells, smart windows, and many other scientific, commercial and consumer products (see for example reference [1] and references therein). In the last years, numerous investigations were carried out to discover new potential n- or p-type TCOs, due to the increasing interest in this class of materials. Most of the TCOs that are suitable for

[a] *Babeş-Bolyai University, Faculty of Chemistry and Chemical Engineering, 11 Arany Janos str., RO-400028, Cluj-Napoca, Romania.*
[*] *Corresponding author: lbizo@chem.ubbcluj*
[b] *Babeş-Bolyai University, Institute for Interdisciplinary Research on Bio-Nano-Sciences, 42 Treboniu Laurian str., RO-400271 Cluj-Napoca, Romania*

practical use are still n-type semiconductors, due to the ease of forming cation interstitials or oxygen vacancies [2]. The important TCO semiconductors are impurity-doped ZnO, $In_2O_3$, and $SnO_2$ as well as multicomponent oxides consisting of combinations of these oxides including some ternary compounds existing in their systems. The $In_2O_3$ with its bixbyite structure and more generally oxygen deficient fluorite type oxides, involving $d^{10}$ cations seem to play a prominent role in the discovery of transparent conductors. Beside the well-known ITO (indium tin oxide), considered the best material for optoelectronic applications, other types of doping or substitutions in indium oxide were intensely studied in the last years [3-13]. Indium and its compounds are considered critical raw materials (CRM) and many efforts are focused on investigating CRM substitution alternatives [14]. However, substitution of flat panel displays containing ITO, either by an ITO alternative or a different display technology, is currently not possible without a loss of performance or the use of another indium containing component.

In this context, reducing the amount of highly expensive and scarce indium oxide by substitutions in indium oxide has to be investigated intensively. For this reason, we decided to check the ability for the substitution of the (Ga/Zr) couple for indium in $In_2O_3$. We hereafter report the results of such an investigation in terms of $In_{2-2x}Ga_xZr_xO_3$ solid solutions, which previously has not been reported. X-ray powder diffraction (XRPD), Scanning Electron Microscopy (SEM) and Energy Dispersive X-ray Spectroscopy (EDS), UV-VIS spectroscopy and electrical resistivity measurements were used to analyze the effect of coupled substitution of $Zr^{4+}/Ga^{3+}$ for $In^{3+}$ in $In_2O_3$ on the structural and physical properties.

## RESULTS AND DISCUSSION

According to the above reported experimental procedure, a new series of compositions belonging to $In_{2-2x}Ga_xZr_xO_3$ solid solution ($0 \le x < 0.15$) were experimented. The X–ray powder diffraction (XRPD) spectra of six compositions were shown in Figure 1(a). All samples have good crystallinity and all of the major reflections could be well indexed to bixbyite-type cubic lattice structure. The extent of the homogeneity range of this solid solution was deduced from the variation of the parameter of their cubic unit cell obtained from the refinement of XRPD data using the bixbyite-based structural model, S.G. $Ia\bar{3}$ (206), with two sets of cationic positions 8(b): ¼, ¼, ¼, 24(d): x, 0, ¼, and one set of oxygen position 48(e): x, y, z [16]. In Figure 1(b) we give as an example the results of the Rietveld refinement of XRPD pattern for a sample with nominal composition $In_{1.9}Ga_{0.05}Zr_{0.05}O_3$. The calculated parameter values are listed in Table 1. As expected from the smaller cationic mean size resulting from the double substitution reaction 2 $In^{3+}$ (0.80 Å) → $Ga^{3+}$ (0.62 Å) + $Zr^{4+}$ (0.72 Å), the value of the *a* parameter decreases with increasing x, which

indicate solubility up to x = 0.15 (Figure 2). Hence, the substitution of $Zr^{4+}/Ga^{3+}$ for $In^{3+}$ in $In_2O_3$ is evident. The lattice parameter no longer changes as the doping level is increased beyond x = 0.15, confirming that the solubility limit is around 7.5 at%. The solubility limits of Ga and Zr in indium oxide are in good agreement with results reported by Edwards et al. and Sasaki et al. [17, 18]. Above this composition (x = 0.15) the *a* parameter remain practically constant and impurity phases identified to both tetragonal and monoclinic $ZrO_2$ starts to appear. It is known that $ZrO_2$ has three polymorphs: monoclinic (m-phase, below 1170 °C), tetragonal (t-phase, between 1170 and 2370 °C) and cubic (c-phase, above 2370 °C) [19, 20].

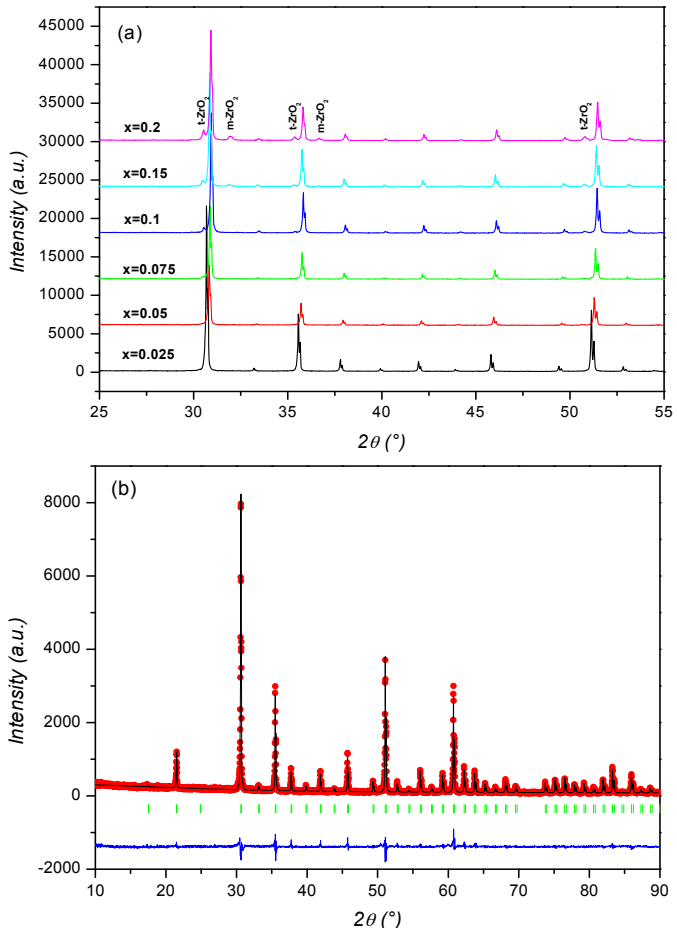


**Figure 1. (a)** XRPD pattern of six compositions belonging to $In_{2-2x}Ga_xZr_xO_3$ system and **(b)** observed (dots), calculated (lines) and difference XRPD pattern of x = 0.05 composition (after heating at 1400 °C).

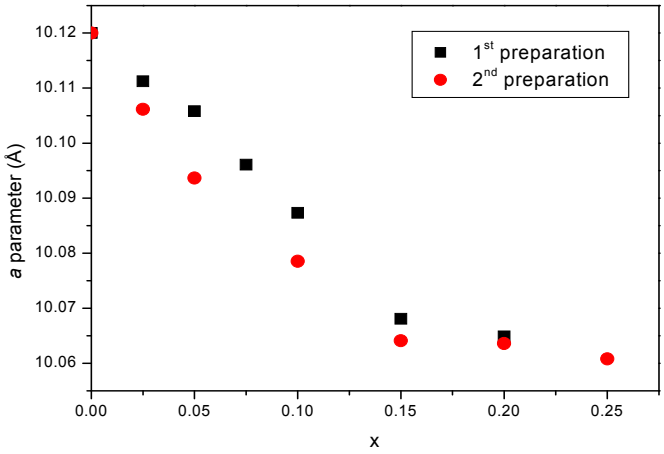


**Figure 2.** Variation of *a* parameter (Å) versus composition x of the cubic unit cell in the $In_{2-2x}Ga_xZr_xO_3$ system.

In order to check the reproducibility of the synthesis procedure, two sets of samples were prepared, using the same preparative method, namely 1st and 2nd preparation, respectively. As observed from Table 1, no major difference of the cell parameters values occurred.

**Table 1.** Values of *a* parameter obtained from Rietveld refinement of XRPD data for two different preparations of the same composition belonging to $In_{2-2x}Ga_xZr_xO_3$ system.

| Composition | *a* [Å] | |
|---|---|---|
| | 1st preparation | 2nd preparation |
| x = 0.025 | 10.11123(11) | 10.106140(10) |
| x = 0.05 | 10.10579(17) | 10.093659(10) |
| x = 0.075 | 10.09609(16) | - |
| x = 0.1 | 10.08734(17) | 10.078545(15) |
| x = 0.15 | 10.0681(2) | 10.0641(2) |
| x = 0.2 | 10.0649(3) | 10.0636(6) |
| x = 0.25 | - | 10.0608(5) |

The surface morphology of x = 0.05 and x = 0.1 compositions appear homogenous and consist of small grains as shown in Figure 3. The grain size ranges from approximately 5 to 15 μm. The results of EDS analysis corresponding to the same nominal cationic compositions highlight the simultaneous presence of the In, Ga and Zr elements and no others was systematically detected. The results for x = 0.05 sample are less definitive as the Ga and Zr content is very small.

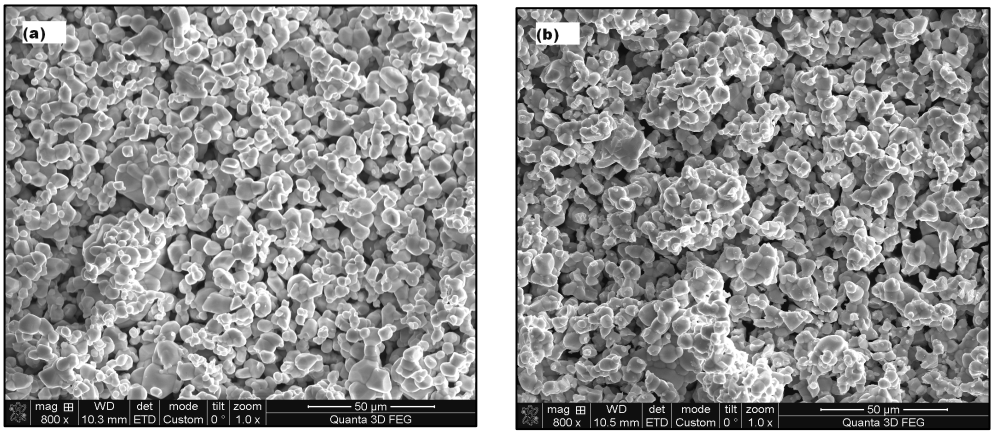


**Figure 3.** SEM images of x = 0.05 (a) and x = 0.1(b) compositions at 800x magnification.

The color of the samples prepared at 1400 °C is medium green. Their measured diffuse reflectance spectra (DRS) are displayed in Figure 4(a) together with the corresponding spectra of an undoped indium oxide ceramic sample annealed at the same temperature. In any case, a systematic decrease of the maximum percent reflectance around 550 nm, if compare to pure indium oxide, was observed. This decrease is more pronounced in the x = 0.075 composition, by approximately 15% with respect to undoped indium oxide. A slight increase of bandgap due to the substitution of $In^{3+}$ ions with $Zr^{4+}$ and $Ga^{3+}$ was observed. This increase of bandgap with doping is well known as a result of the Burstein-Moss effect that occurs in degenerate doped semiconductors [21].

Regarding the influence of firing temperature on optical properties, DRS spectra for x = 0.05 sample were recorded after three heating treatments, 1200 °C, 1300 °C and 1400 °C, respectively. As visible from Figure 4(b), the maximum percent reflectance is lowered by 18 % at increasing temperature from 1200 °C to 1400 °C. It is clear that bandgap increases with increasing annealing temperature and its maximum value of 3.306 eV is obtained at a temperature of 1400 °C. The increase in optical bandgap may be related to the improvement of sample crystallinity. On the other hand, the optical band gap broadening with increasing firing temperature can be described in terms of Burstein-Moss model. Moreover, in the case of degenerated semiconductors the optical bandgap is influenced by changes in the carrier concentration, which blocks the lowest states of the bottom of the conduction band, resulting in the Burstein–Moss shift. As the firing temperature increases, the absorption edge shifts to longer wavelengths.

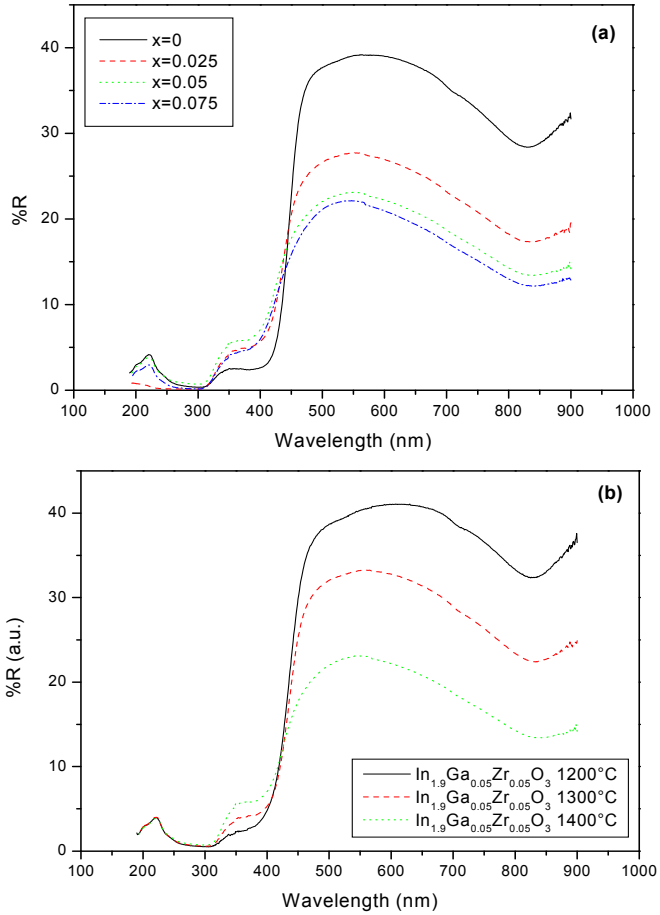


**Figure 4.** DRS spectra for x = 0.025, x = 0.05, x = 0.075 compositions and $In_2O_3$ (x = 0) for comparison (a) and x = 0.05 composition treated at three different temperatures (b).

The temperature dependence of the electrical resistivity of the three compositions of $In_{2-2x}Ga_xZr_xO_3$ solid solution (x = 0.025, x = 0.05 and x = 0.075) and indium oxide for comparison is displayed in Figure 5. Within the whole temperature range 5-320 K a semi-metallic behavior of the (Ga/Zr) compositions is observed. In any case, the introduction of the cationic couples (Ga/Zr) in $In_2O_3$ triggers systematically a decrease of the resistivity if compare to $In_2O_3$. The best value of resistivity obtained for the x = 0.025 compositions, $\rho_{RT}$ = 5 x $10^{-3}$ Ω.cm, is lowered by almost one order of magnitude compared to bulk $In_2O_3$. It should be emphasized that this resistivity value is comparable to that of an ITO ceramic sample (3% Sn) prepared at the same temperature (1400 °C), in air ($\rho_{RT}$ = 0.5 x $10^{-3}$ Ω.cm) [22].

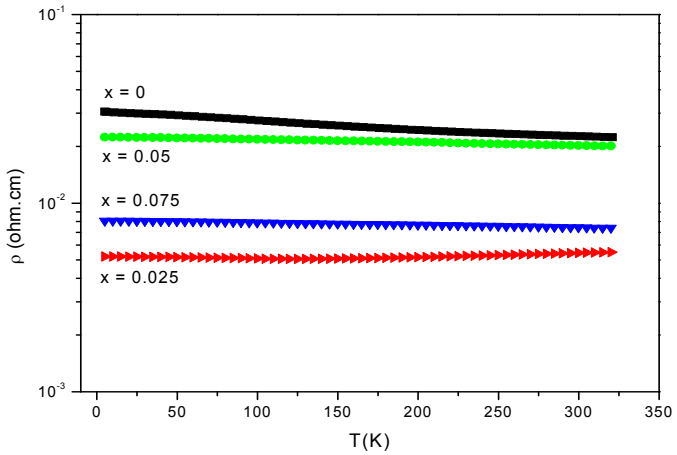


**Figure 5.** Electrical resistivity (ohm.cm) versus temperature (K) for x = 0.025, x = 0.05 and x = 0.075 compositions and compared with $In_2O_3$ (x = 0).

## CONCLUSIONS

Different compositions belonging to the $In_{2-2x}Ga_xZr_xO_3$ system have been successfully synthesized by the solid-state reaction method. X-ray powder diffraction (XRPD) technique used for phase analysis and structure calculation verified that all samples exhibited a single bixbyite structure up to x = 0.15. The homogeneity of the substitution procedure $2In^{3+} \rightarrow Zr^{4+}+Ga^{3+}$ was confirmed. The maximum percent reflectance around 500 nm is lowered by 15% with respect to pure $In_2O_3$. The optical bandgap is somewhat shifted towards the lower wavelengths, i.e. the larger energies. A decrease of room temperature resistivity for the composition x = 0.025 ($\rho_{RT}$ = 5.5x10$^{-3}$ Ω.cm) was observed, which is approximately one order of magnitude less than undoped $In_2O_3$ ($\rho_{RT}$ = 2.2x10$^{-2}$ Ω.cm). The coupled substitution of the (Ga/Zr) for In promotes a good level of conductivity of the bulk materials together with a satisfying optical transparency as compared to pure indium oxide prepared under the same conditions. We can conclude that these novel oxides are promising candidates as transparent conducting oxides for optoelectronic applications.

## EXPERIMENTAL SECTION

### Samples preparation

The different compositions of $In_2O_3$:(Zr, Ga) oxides were prepared by solid state reaction in air. The raw materials were pure oxides of $In_2O_3$

(Alfa Aesar 99.995%), $ZrO_2$ (Alfa Aesar 99%) and $Ga_2O_3$ (Alfa Aesar 99.999%). The oxide mixture was milled using an agate mortar and then heated in an alumina crucible using a high-temperature Nabertherm LHT 04/16 furnace. Successive 12h heating temperature, from 600 °C up to 1400 °C, followed by air quenching and regrinding were performed. The samples preparation was repeated ($1^{st}$ and $2^{nd}$ preparation). Multiple samples were prepared at the x = 0.025, x = 0.05, x = 0.075, x = 0.1, x = 0.15 and x = 0.2 compositions in order to test the reproducibility of the preparation procedure (Table 1).

**Characterization methods**

X-ray powder diffraction (XRPD) was used for phase analysis and further for structure calculations. The diffractograms were recorded on a Panalitcal X'Pert diffractometer (CuKα1 radiation), equipped with an X'Celerator detector, in the angular range 2θ = 6-120°. A Rietveld analysis (Fullprof code [15]) of the diffractograms was systematically performed.

UV–VIS diffuse reflectance spectra (DRS) of the as-prepared compositions were determined by a double beam spectrophotometer (Cary Varian 100 Scan), in the range 190-900 nm with a 600 nm/min scan rate.

The electrical resistivity of pellets sintered at 1400 °C in the air was measured by the four-probe method in the range of 5-320 K, using a PPMS (Physical Properties Measurements System) device.

The samples morphology was investigated using an FEI Quanta 3D FEG dual beam microscope in scanning electron microscopy (SEM) mode. Chemical analysis of local area was carried out by energy dispersive X-ray spectroscopy (EDS) measurements performed on the same microscope.

## REFERENCES


**1.** D. S. Ginley, H. Hosono, D. C. Paine, "Handbook of Transparent Conductors", Springer, Berlin, **2010.**
2. S. Lany, A. Zunger, Dopability, *Physical Reviews Letters*, **2007**, *98*, 0455011.
3. L. Bizo J. Choisnet, R. Retoux, B. Raveau, *Solid State Communications,* **2005**, *136*, 163.
4. L. Bizo, J. Choisnet, B. Raveau, *Materials Research Bulletin*, **2006**, *41*, 2232.
5. J. Choisnet, L. Bizo, R. Retoux, B. Raveau, *Solid State Science*, **2004**, *6*, 1121.
6. D. Berardan, E. Guilmeau, A. Maignan, B. Raveau, *Solid State Communications*, **2008**, *146*, 97.

7. F. Nanni, F. R. Lamastra, F. Franceschetti, F. Biccari, I. Cacciotti, *Ceramics International*, **2014**, *40*, 1851.
8. T. Asikainen, M. Ritala, M. Leskela, *Thin Solid Films*, **2003**, *440*, 152.
9. H. K. Kim, C. C. Li, G. Nykolak, P.C. Becker, *Journal of Applied Physics,* **1994**, *76*, 8209.
10. T. Koida, M. Kondo, *Applied Physics Letters*, **2006**, *89*, 0821041.
11. Y.-C. Liang, Y.-C. Liang, *Applied Physics A-Material Science*, **2009**, *97*, 249.
12. H. J. Chun, Y. S. Choi, S. Y. Bae, H. C. Choi, J. Park, *Applied Physics Letters*, **2004**, *85*, 461-464.
13. J.-H. Lim, E.-J. Yang, D.-K. Hwang, J.-Ho Yang, J.-Y. Oh, S.-J. Park, *Appl. Phys. Lett.,* **2005**, *87*, 0421091.
14. European Commission, Report on Critical Raw Materials for the EU, **2014**.
15. J. Rodriguez-Carvajal, T. Roisnel, Proc. 8-th European Powder Diffraction Conference (EPDIC) 8, Uppsala, Sweden, Ed. Y. Andersson, E. J. Mittemeijer, U. Welze, Trans Tech Publications Ltd, Switzerland, **2004**, 123.
16. N. Nanaud, N. Lequeux, M. Nanot, *Journal of Solid State Chemistry*, **1998**, *135*, 140.
17. D. D. Edwards. P. E. Folkins, T. O. Mason, *Journal of American Ceramic Society*, **1997**, *80*, 253.
18. T. O. Mason G. B. González, J.-H. Hwang, D. R. Kammler, *Physical Chemistry Chemical Physics*, **2003**, *5*, 2183.
19. T. Chraska, A. H. King, C. C. Berndt, *Materials Science and Engineering: A*, **2000**, *286*, 169.
20. T. Y. Luo, T. X Liang, C. S. Li, *Materials Science and Engineering: A,* **2004**, *366*, 206.
21. E. Burstein, *Physical Reviews*, **1954**, *93*, 632.
22. Ambrosini, A. Duarte, K. R. Poeppelmeier, M. Lane, K. N. Kannewurf, T. O. Mason, *Journal of Solid State Chemistry*, **2000**, *153*, 41.